Collisional excitation by electrons of the heavy alkali-metal-like ion Sr^+

M. C. Chidichimo
Department of Applied Mathematics, University of Waterloo, Waterloo, Ontario, Canada N2L 3G1
(Received 14 June 1988)

Total cross sections and collision strengths for the 5*s*-5*p*, 4*d*-5*p*, and 5*s*-4*d* transitions in Sr^+, calculated in the Coulomb distorted-wave, Coulomb-Born, and Coulomb-Bethe approximations, are presented. The calculations have been carried out using a unitarized three-state approximation (5*s*-4*d*-5*p*) and in the *LS* coupling scheme, for the incident energy range 3–300 eV. The model for alkali-metal ions, of a single outer electron, has been considered, and exchange between the optical and incident electron neglected. The collision strengths have been processed using a new method for interpolating and assessing collision strengths, which allows data to be extrapolated correctly up to high energies. This new approach confirms the high-energy behavior shown in the present data.

I. INTRODUCTION

Excitation of heavy alkali-metal-like ions by electron collisions plays an important role in the modeling of physical processes taking place in cool stars with excesses of heavy elements.[1,2] We have calculated the 5*s*-5*p*, 4*d*-5*p*, and 5*s*-4*d* excitation cross section of Sr^+ between threshold and 300 eV, using a unitarized three-state approximation. Sr^+ has an energy-level structure which might be appropriate for this type of approach, since it has a small group of low-lying states (5*s*-4*d*-5*p*) fairly well separated from the rest. We have used the Coulomb distorted-wave (CDW), Coulomb-Born (CB), and Coulomb-Bethe (CBe) approximations in the *LS* representation, omitting exchange between the atomic and incident electrons. We have described already these calculation techniques in detail in connection with the excitation of the Mg^+ ion[3] and the Ca^+ ion.[4] Therefore, only a brief description of our method is given in Sec. II. To the best of our knowledge, these are the first reported calculations of excitation cross sections for the 5*s*-4*d* and 4*d*-5*p* transitions. Previous theoretical calculations have dealt with the 5*s*-5*p* resonant transition.[5] The information available on experimental excitation cross sections unfortunately is scarce. There has been only one experiment on the emission cross section of the resonant line of Sr^+, carried out by Zapesochnyi and co-workers.[6] In Sec. III we discuss our method of obtaining bound-state wave functions. In Sec. IV we present our results and compare them with other theoretical calculations and experiments, and Sec. V contains the conclusions. We have used atomic units throughout this paper, except for energies where we have used Rydberg units.

II. THEORY

The excitation cross section $Q(nl_a \rightarrow n'l'_a)$ of alkali-metal-like positive ions for the transition $nl_a \rightarrow n'l'_a$ can be expressed in terms of the collision strength $\Omega(n'l'_a, nl_a)$ by the equation

$$Q(nl_a \rightarrow n'l'_a) = \frac{\Omega(n'l'_a, nl_a)}{(2l_a+1)E}(\pi a_0^2) , \tag{1}$$

where $(2l_a+1)$ is the statistical weight of the initial level nl_a and E is the impact electron energy in Rydbergs. Notice that the spin statistical-weight factor of 2 has been omitted in the degeneracy of the initial level nl_a. The ion, with nuclear charge Z_0 and N electrons, is assumed to have a frozen core with $(N-1)$ electrons. In the coupled angular momentum representation the total collision strength $\Omega(n'l'_a, nl_a)$ is related to the transmission T^A matrix by

$$\Omega(n'l'_a, nl_a) = \sum_{L=0}^{\infty} \Omega_L , \tag{2}$$

where

$$\Omega_L = \sum_{l,l'} (2L+1)|T^A(n'l'_a k'l'L, nl_a klL)|^2 , \tag{3}$$

and A ($\equiv$CDW, CB or CBe) denotes the approximation in which the $\underline{T}$ matrix has been evaluated. nl_a are the principal quantum numbers of the atomic electron (valence electron) and specify a target state, k and l are, respectively, the wave number and orbital angular momentum of the colliding electron, and L is the total orbital angular momentum of the system (ion plus incident electron). The transmission matrix $\underline{T}$ is related to the matrix $\underline{\mathcal{T}}$ by[3]

$$T(\gamma', \gamma) = \mathcal{T}(\gamma', \gamma) \quad \text{for } \gamma' \neq \gamma , \tag{4}$$

$$T(\gamma', \gamma) = 1 + \exp(2i\tau_\gamma)[\mathcal{T}(\gamma', \gamma) - 1] \quad \text{for } \gamma' = \gamma , \tag{5}$$

where γ denotes $nl_a klL$ and specifies the scattering channels in an *LS* coupling representation. $T(\gamma', \gamma)$ may be evaluated in the CDW, CB, and CBe approximations. In the CB or CBe approximation the phase shift $\tau_\gamma = 0$ [see Eqs. (15) and (16)] and hence $\underline{T} \equiv \underline{\mathcal{T}}$. The transmission matrix $\underline{T}$ is related to the reactance matrix $\underline{R}$ by

$$\underline{T} = \frac{-2i\underline{R}}{\underline{1} - i\underline{R}} , \tag{6}$$

and a similar relation holds between the matrix $\underline{T}$ and matrix $\underline{\rho}$,

$$\underline{T} = \frac{-2i\underline{\rho}}{\underline{1} - i\underline{\rho}} . \tag{7}$$

We refer to these unitarization schemes as approximation II (strong coupling). If $\underline{R}(\underline{\rho}) \ll 1$, which is valid only in the weak coupling case, the $\underline{T}(\underline{\mathcal{T}})$ matrix can be written as

$$\underline{T} \simeq -2i\underline{R} \quad \text{and} \quad \underline{\mathcal{T}} \simeq -2i\underline{\rho} \ , \tag{8}$$

which is referred to as approximation I (weak coupling).

A. Coulomb distorted-wave approximation

In this approximation, allowance is made for the effect of the short-range and long-range static field of the atomic system on the incident and scattered Coulomb waves. The CDW matrix element $\rho(\gamma',\gamma)$ is given by

$$\rho^{\mathrm{CDW}}(\gamma',\gamma) = -\int_0^\infty F_{\gamma}^{\mathrm{CDW}}(r) W_{\gamma\gamma'}(r) F_{\gamma}^{\mathrm{CDW}}(r) dr \ , \tag{9}$$

with the collisional potential

$$\begin{aligned} W_{\gamma\gamma'} = 2 \Big[& [1-\delta(n,n')]\delta(l_a l, l_a' l') s_0(P_{nl_a} P_{n'l_a'} | r) \\ & + [1-\delta(nl_a l, n' l_a' l')] \\ & \times \sum_{\lambda>0} f_\lambda(l_a l, l_a' l'; L) y_\lambda(P_{nl_a} P_{n'l_a'} | r) \Big] \ , \end{aligned} \tag{10}$$

γ denotes $nl_a lL$, $P_{nl_a}(r)$ are the target bound-state wave functions, the angular coefficients f_λ are tabulated algebraic quantities,[7]

$$\begin{aligned} y_\lambda = & \frac{1}{r^{\lambda+1}} \int_0^r P_{n'l_a'}(\xi) \xi^\lambda P_{nl_a}(\xi) d\xi \\ & + r^\lambda \int_r^\infty P_{n'l_a'}(\xi) \xi^{-\lambda-1} P_{nl_a}(\xi) d\xi \end{aligned} \tag{11}$$

is the usual multipole potential,[7] and $s_0(P_{nl_a}, P_{n'l_a'} | r)$ is a short-range interaction term given by

$$\begin{aligned} s_0(P_{nl_a}, P_{n'l_a'} | r) = & \int_r^\infty P_{n'l_a'}(\xi) \xi^{-1} P_{nl_a}(\xi) d\xi \\ & - \frac{1}{r} \int_r^\infty P_{n'l_a'}(\xi) P_{nl_a}(\xi) d\xi \ . \end{aligned} \tag{12}$$

$F_{\gamma}^{\mathrm{CDW}}(r)$ satisfies the equation

$$\left[\frac{d^2}{dr^2} - \frac{l(l+1)}{r^2} + \frac{2(z-1)}{r} + V_\gamma(r) + k_\gamma^2 \right] F_{\gamma}^{\mathrm{CDW}}(r) = 0 \ , \tag{13}$$

with boundary conditions

$$F_{\gamma}^{\mathrm{CDW}}(r) \sim 0, \quad r \to 0 \tag{14}$$

$$F_{\gamma}^{\mathrm{CDW}}(r) \sim k_\gamma^{-1/2} \sin(\zeta_\gamma + \tau_\gamma), \quad r \to \infty \tag{15}$$

where $z = Z_0 - N + 1$ is the atomic charge seen by the atomic electron (core charge) and $k_\gamma^2 = E_T + \varepsilon_{nl_a}$, where E_T is the total energy of the system (ion$+e$). $E_T = 0$ corresponds to the frozen core plus two free electrons of zero kinetic energy and ε_{nl_a} is the binding energy of the atomic state specified by the quantum numbers nl_a. τ_γ is the phase shift due to the static potential

$$V_\gamma(r) = 2 \left[\frac{Z^{\mathrm{eff}}(r)}{r} - s_0(P_{nl_a}, P_{nl_a} | r) - \sum_{\lambda>0} f_\lambda y_\lambda \right] , \tag{16}$$

where $Z^{\mathrm{eff}}(r)/r - s_0(P_{nl_a}, P_{nl_a} | r)$ is a local, central short-range potential, which accounts for the ion core and $-\sum_{\lambda>0} f_\lambda y_\lambda$ terms may include long-range even multipole contributions, corresponding to the γ channel. The sum over λ (for $\lambda > 0$) in the $\rho^{\mathrm{CDW}}(\gamma',\gamma)$ matrix [Eq. (9)] has a finite number of terms, which may include dipole ($\lambda = 1$) and multipole transitions ($\lambda > 1$).

The function $Z^{\mathrm{eff}}(r)$ measures the increase in nuclear charge as an electron penetrates the core: $Z^{\mathrm{eff}}(\infty) = 0$, $Z^{\mathrm{eff}}(0) = N - 1$ and is defined in Sec. III:

$$\zeta_\gamma = k_\gamma r - \frac{l\pi}{2} + \frac{(z-1)}{k_\gamma} \ln(2k_\gamma r) + \sigma_l \ , \tag{17}$$

with

$$\sigma_l = \arg\Gamma \left[l + 1 - i\frac{(z-1)}{k_\gamma} \right] . \tag{18}$$

B. Coulomb-Born and Coulomb-Bethe approximations

The Coulomb-Born reactance matrix element is given by

$$R^{\mathrm{CB}}(\gamma',\gamma) = -\int_0^\infty F_\gamma(r) W_{\gamma\gamma'}(r) F_{\gamma'}(r) dr \ , \tag{19}$$

where $F_\gamma(r)$ is a regular Coulomb function and

$$W_{\gamma\gamma'} = 2 \left[\left[-\frac{Z^{\mathrm{eff}}(r)}{r} \delta(n,n') + s_0(P_{nl_a}, P_{n',l_a'} | r) \right] \delta(l_a l, l_a' l') + \sum_{\lambda>0} f_\lambda(l_a l, l_a' l'; L) y_\lambda(P_{nl_a}, P_{n'l_a'} | r) \right] . \tag{20}$$

In the Coulomb-Bethe approximation it is assumed that only the long-range part of the interaction is important. So that, using

$$y_\lambda(r) \sim \frac{1}{r^{\lambda+1}} \int_0^\infty P_{n'l_a'}(r) r^\lambda P_{nl_a}(r) dr \ , \tag{21}$$

the $R^{\mathrm{CBe}}(\gamma',\gamma)$ matrix element is given by Eq. (19) with

$$W_{\gamma\gamma'} = 2 \sum_{\lambda>0} f_\lambda(l_a l, l_a' l'; L) \frac{1}{r^{\lambda+1}} \int_0^\infty P_{n'l_a'}(r) r^\lambda P_{nl_a}(r) dr \ . \tag{22}$$

C. Contribution to the collision strength from large values of the angular momentum

Equation (2) may be rearranged as

$$\Omega(n'l'_a,nl_a)=\sum_{l=0}^{\infty}\sum_{l'}\Omega_{l'l}\ , \tag{23}$$

where

$$\Omega_{l'l}=\sum_{L}(2L+1)|T(n'l'_ak'l'L,nl_aklL)|^2\ . \tag{24}$$

At high incident energies and for optically allowed ($\lambda=1$) and optically forbidden ($\lambda=2$) transitions, the sum over l in Eq. (23) is slowly convergent. We have split the infinite sum in Eq. (23) into two parts,

$$\Omega(n'l'_a,nl_a)=\Omega_{l_0}+\tilde{\Omega}_{l_0+1}\ , \tag{25}$$

where

$$\Omega_{l_0}=\sum_{l=0}^{l_0}\sum_{l'}\Omega_{l'l}\ , \tag{26}$$

and

$$\tilde{\Omega}_{l_0+1}=\sum_{l=l_0+1}^{\infty}\sum_{l'}\Omega_{l'l}^{\mathrm{CBe\,I}}\ . \tag{27}$$

The sum from $l=0$ to $l=l_0$ has been evaluated in the CDW II, CB II, or CBe II approximations and the sum from $l=l_0+1$ to ∞ has been estimated using the CBe I approximation. By choosing a high enough value l_0, the ratio $\Omega_{l'l}/\Omega_{l'l}^{\mathrm{CBe\,I}}$ can be made as near to unity as desired. Typical values of l_0 are $l_0=15$ for an incident electron energy $k_{5s}^2=0.22444$ Ry, and $l_0=55$ for $k_{5s}^2=22.443$ Ry. For the $5s$-$5p$ and $5p$-$4d$ dipole transitions the contributions $\tilde{\Omega}_{l_0+1}$ were evaluated using the analytic formula of Burgess.[5,8] In the case of the $5s$-$4d$ quadrupole transition, two methods, each of them suitable in a different range of the incident electron energy, have been used to evaluate the infinite sums in Eqs. (2) or (27). For low incident electron energies, such as from threshold to 2.2443 Ry, the usual geometric series method has been applied. The infinite sum in Eq. (2) has been split into two parts,

$$\Omega(4d,5s)=\sum_{L=0}^{L_0}\Omega_L+\sum_{L=L_0+1}^{\infty}\Omega_L\ , \tag{28}$$

in which a value L_0 has been found such that

$$\frac{\Omega_L}{\Omega_{L-1}}=a=\text{const}\quad\text{for } L\geq L_0\ , \tag{29}$$

hence

$$\sum_{L=L_0+1}^{\infty}\Omega_L=\Omega_{L_0+1}\sum_{t=0}^{\infty}a^t=\frac{\Omega_{L_0+1}}{1-a}\ . \tag{30}$$

Illustrative examples are, for $k_{5s}^2=0.45627$ Ry, $L_0=25$ and $a=0.703$, and for $k_{5s}^2=2.2443$ Ry, $L_0=45$ and $a=0.924$. At energies greater than 2.2443 Ry the previous method becomes impractical because the ratio Ω_L/Ω_{L-1} converges extremely slowly to a constant value as L becomes large. At these higher energies an analytic method has been developed,[3] in which the assumption has been made that $k\sim k'$ and $l\gg 1$. The contribution $\tilde{\Omega}_{l_0+1}$ to the total collision strength Ω for this range of energies and angular momentum is given by

$$\tilde{\Omega}_{l_0+1}=\tfrac{16}{5}B^2(5s,4d;2)(z-1)^2S_{l_0+1}\ , \tag{31}$$

where

TABLE I. Total collision strength Ω in the CDW II approximation for the $5s$-$4d$ transition. The contribution Ω_{l_0} and $\tilde{\Omega}_{l_0+1}$ to Ω are shown separately, together with error estimates.

E(Ry)	l_0	Ω_{l_0}	$\tilde{\Omega}_{l_0+1}$	Ω	$\tilde{\Omega}_{l_0+1}$ as percentage of Ω	Percentage absolute error in Ω
4.0	15	4.412	8.728×10^{-1}	5.285	17	2
	30	5.112	2.128×10^{-1}	5.325	4	2
	40	5.219	1.181×10^{-1}	5.337	2	1
6.7329	11	2.894	2.713	5.607	48	9
	25	4.655	5.164×10^{-1}	5.171	10	2
	33	4.890	2.940×10^{-1}	5.184	6	2
	50	5.073	1.257×10^{-1}	5.199	2	1
12.0	15	2.938	2.555	5.493	47	7
	29	4.447	6.786×10^{-1}	5.126	13	1
	44	4.843	2.910×10^{-1}	5.134	6	<1
	59	4.982	1.590×10^{-1}	5.141	3	<1
22.443	15	2.035	4.736	6.771	70	34
	29	3.843	1.265	5.108	25	1
	44	4.531	5.434×10^{-1}	5.074	11	<1
	55	4.731	3.437×10^{-1}	5.075	7	<1

$$B(5s,4d;2)=\int_0^\infty P_{5s}(r)r^2P_{4d}(r)dr\ , \tag{32}$$

$$S_{l_0+1}\approx a_3(\bar\kappa)\sum_{l=l_0+1}^{\infty}\frac{1}{l^3}+a_4(\bar\kappa)\sum_{l=l_0+1}^{\infty}\frac{1}{l^4}+a_5(\bar\kappa)\sum_{l=l_0+1}^{\infty}\frac{1}{l^5}\ , \tag{33}$$

$$a_3(\bar\kappa)=\frac{\bar\kappa^2}{6}\ , \tag{34}$$

$$a_4(\bar\kappa)=\frac{\bar\kappa\pi}{4}(1-e^{-2\pi/\bar\kappa})^{-1}\ , \tag{35}$$

$$a_5(\bar\kappa)=\frac{\pi^2}{8}(1-e^{-2\pi/\bar\kappa})^{-2}\ , \tag{36}$$

$$\bar\kappa=\frac{1}{(z-1)}\left[\frac{k^2+k'^2}{2}\right]^{1/2}\ , \tag{37}$$

and $z-1=1$ for single ionized ions. For the energies considered, the coefficients $a_3(\bar\kappa)$, $a_4(\bar\kappa)$, and $a_5(\bar\kappa)$ are always less than 6.0. The error term $(\sum_{l=l_0+1}^{\infty} l^{-M}-\sum_{l=l_0+1}^{l_{\max}} l^{-M})$ is $O(l_{\max}^{-M+1})$, so we summed the series in Eq. (30) to $l_{\max}=300$ to obtain their values correct to four decimal places. Equation (32) gives the value $B(5s,4d;2)=-13.44$ for the transition $5s$-$4d$. We show in Table I, for the transition $5s$-$4d$ and at each incident electron energy, the two contributions Ω_{l_0} (in the CDW II approximation) and $\tilde\Omega_{l_0+1}$, to the total collision strength Ω for various angular momenta. The percentage contribution to $\tilde\Omega_{l_0+1}$ to Ω is also shown as well as an estimate of the percentage error in Ω due to the use of the analytic formula (31). The error estimate is only for this effect, not for the CDW II approximation which is of the order of 1%. The procedure followed to obtain an estimate of this error has been explained in detail in a previous paper.[3]

III. TARGET ION: Sr^+

The radial orbitals $P_i(r)$ for the target ion satisfy the equation

$$\left[\frac{d^2}{dr^2}-\frac{l_i(l_i+1)}{r^2}+\frac{2z}{r}+2\frac{Z_i^{\rm eff}(\alpha|r)}{r}-\varepsilon_i\right]P_i(r)=0\ , \tag{38}$$

where $\varepsilon_i=I-E_i$ is the observed binding energy of an electron in subshell i. $I=88\,964.0\ \mathrm{cm}^{-1}$ is the ionization energy of the valence electron and E_i are the term energies of Sr^+.[9] The experimental energies quoted are weighted means of terms belonging to the same configuration given by

$$E_i=\frac{1}{2(2l_i+1)}\sum_{j=l_i-1/2}^{j=l_i+1/2}(2j+1)E_{ij}\ . \tag{39}$$

Nonlinear scaling parameters in the function $Z_i^{\rm eff}(\alpha|r)$ are adjusted so that the correct experimental energy is obtained as part of the solution of Eq. (38). It is assumed that each electron moves independently in a potential which is generated by the nuclear charge Z_0 and the charge distribution of the other electrons. For an N-electron ion with nuclear charge Z_0, N_s atomic subshells, and with q_j electrons in each subshell j, the potential of an electron in subshell i is given in terms of $Z_i^{\rm eff}(\alpha|r)$ by the equation

$$\frac{Z_0}{r}-\sum_{j=1}^{N_s}(q_j-\delta_{ij})Y_0(P_{n_j}^{\rm STO}|r)=\frac{z}{r}+\frac{Z_i^{\rm eff}(\alpha|r)}{r}\ , \tag{40}$$

where α stands for the set of scaling parameters,

$$Y_0(P|r)=\frac{1}{r}\int_0^r P^2(\xi)d\xi+\int_r^\infty P^2(\xi)\frac{d\xi}{\xi}\ , \tag{41}$$

and

$$P_{n_j}^{\rm STO}(r)=\frac{1}{\sqrt{(2n_j)!}}\left[\frac{2Z_j\alpha_j}{n_j}\right]^{n_j+1/2}r^{n_j}\exp\left[\frac{Z_j\alpha_j r}{n_j}\right] \tag{42}$$

are Slater-type orbitals (STO) which are used to compute the average screening by electrons in subshell j, with

$$Z_j=Z_0-\sum_{t=1}^{j-1}q_t-\tfrac{1}{2}(q_j-1)\ , \tag{43}$$

n_j the principal quantum number of subshell j, and α_j an adjustable scaling parameter. $Z_i^{\rm eff}(\alpha|r)$, which is short range, has the following analytical form:[10]

$$Z_i^{\rm eff}(\alpha|r)=(N-1)-\sum_{j=1}^{N_s}(q_j-\delta_{ij})\left\{1-\exp(-\rho_j)\left[\sum_{m=0}^{2n_j-1}\left[\frac{2n_j-m}{2n_jm!}\right]\rho_j^m\right]\right\}\ , \tag{44}$$

with

$$\rho_j=2Z_j\alpha_j r/n_j\ . \tag{45}$$

In the preceding equation we have adopted a more compact notation which does not show that α_j and ρ_j also depend on i. This potential has the important property that the right-hand side of Eq. (44) can be expressed as a power series in r with an infinite radius of convergence.

We have assumed that the core, which has $N-1=36$ electrons and $N_s=8$ subshells, is frozen during the collision and therefore that we require only orbitals for the outer valence electron. These orbitals are solutions of (38) with $Z_i^{\rm eff}(\alpha|r)\equiv Z_{nl_a}^{\rm eff}$ which includes the scaling parameters $\alpha_1=0.013\,92$ and $\alpha_j=1.656\,13$ for $j=2,\ldots,8$. All of the orbitals $nl_a=5s$, $4d$, and $5p$ have been calculated using the same α set (given above) and therefore the

TABLE II. Binding energies and σ^2 of Sr^+.

	ε_{nl_a} (Ry)					
State	Theory[a]	Observed[b]	Transition	Theory[c]		Experiment[d]
$5s$	0.810 79	0.810 70	$5s \rightarrow 5p$	5.64	4.76	4.7 ±0.2
$4d$	0.676 52	0.676 52	$4d \rightarrow 5p$	0.60		0.55±0.1
$5p$	0.586 36	0.589 72				

[a]Present results
[b]Reference 9.
[c]Present results, Burgess and Sheorey (Ref. 5).
[d]Reference 11.

same $Z^{\text{eff}}(r)$. In Table II our theoretical binding energies are compared with the spectroscopic binding energies.[9] Also shown is the quantity

$$\sigma^2 \text{ (a.u.)} = \frac{1}{4l_{a>}^2 - 1} \left| \int_0^\infty P_{n'l'_a}(r) r P_{nl_a}(r) \right|^2 , \quad (46)$$

where $l_{a>}$ is the greater of l_a and l'_a, computed from wave functions obtained using the $Z^{\text{eff}}(r)$ described above. The values of σ^2 obtained for the resonance line and the transition $5p$-$4d$ are compared with Burgess and Sheorey's theoretical result[5] and with those experimentally deduced by Gallagher.[11] Our value of σ^2, for the transition $5s$-$5p$, is slightly larger than the value derived from experimental data. Burgess and Sheorey, in order to get good agreement with the σ^2 obtained from experiment, adjusted the binding energies for the $5s$ and $5p$ states, while keeping the transition energy the same as that obtained from spectroscopic data.

IV. RESULTS

Total collision strengths, for excitations of the $5s$-$5p$, $4d$-$5p$, and $5s$-$4d$ transitions, obtained using a unitarized three-state CDW II, CB II, and CBe II approximation are presented in Tables III and IV. The new method of Burgess *et al.*[12] for interpolating and assessing collision strengths has been used to treat Ω, in the CDW II approximation, for the optically allowed $5s$-$5p$ and $4d$-$5p$ transitions and the $5s$-$4d$ transition. An interactive program with graphical display for the application of this method has been developed by Burgess.[13] By suitable scaling of the collision strength and colliding electron energy [mapped onto the interval (0,1)], the entire variation of Ω is represented on a single graph or table. The scaled Ω is usually represented to a good accuracy ($< 1\%$) by a five-point cubic spline, which simplifies considerably the storage of data, since only five points are needed to reproduce Ω in its entire range. For the optically allowed transitions $5s$-$5p$ and $4d$-$5p$ the Ω varies at high energies as $\Omega \sim \text{const} \times \ln(E)$ and the data are reduced as[12]

$$E_{\text{red}} = 1 - \ln(c)/\ln(E_j/E_{ij} + c) , \quad (47)$$

$$\Omega_{\text{red}} = \Omega/\ln(E_j/E_{ij} + e) , \quad (48)$$

where E_j is the energy of the colliding electron after excitation, E_{ij} is the transition energy, and c is an adjustable parameter chosen to optimize the distribution of data

TABLE III. Total collision strength for the $5s$-$5p$ and $4d$-$5p$ transitions in Sr^+. Energy of the colliding electron after excitation E_j (Ry). ΔE equals transition energy (Ry).

	$5s$-$5p$ $\Delta E = 0.224\,43$			$4d$-$5p$ $\Delta E = 0.090\,16$		
E_j	CDW II	CB II	CBe II	CDW II	CB II	CBe II
1.0×10^{-5}	8.373	10.33	13.25	33.0	26.12	31.72
8.98×10^{-3}	8.851	10.75	13.72	34.08	27.28	33.05
6.957×10^{-2}	11.96	13.43	16.75	40.53	34.34	41.38
1.431×10^{-1}	15.50	16.42	20.18	46.89	41.50	50.12
2.318×10^{-1}	19.27	19.59	23.86	53.03	48.69	59.22
3.619×10^{-1}	24.47	24.11	29.10	59.91	57.28	70.47
4.489×10^{-1}	27.11	26.55	31.98	63.43	62.03	76.97
5.756×10^{-1}	30.88	30.30	36.37	67.71	68.04	85.36
7.756×10^{-1}	35.43	35.25	42.23	73.53	75.76	96.63
1.276×10^{-1}	45.35	45.09	54.04	87.66	89.54	117.93
2.020	56.73	55.29	66.61	103.89	102.69	139.69
3.776	73.10	71.17	87.34	122.89	120.54	172.95
6.508	86.33	84.76	105.90	137.30	135.57	205.36
1.178×10	101.10	100.00	126.40	152.40	151.40	245.50
2.222×10	116.3	115.7	147.80	168.20	167.70	296.60

TABLE IV. Total collision strength for the $5s$-$4d$ transition in Sr^+. Energy of the colliding electron after excitation E_j (Ry). Transition energy equals 0.134 27 Ry.

E_j	CDW II	$5s$-$4d$ CB II	CBe II
1.0×10^{-5}	3.538	2.316	6.689
1.0×10^{-2}	3.648	2.352	6.810
9.017×10^{-2}	4.7	3.968	6.088
9.914×10^{-2}	4.789	3.976	6.130
1.597×10^{-1}	5.286	4.027	6.413
2.332×10^{-1}	5.684	4.077	6.733
3.220×10^{-1}	5.925	4.118	7.063
4.521×10^{-1}	5.985	4.187	7.553
5.390×10^{-1}	5.915	4.200	7.791
6.657×10^{-1}	5.803	4.246	8.193
8.657×10^{-1}	5.722	4.279	8.712
1.366	5.704	4.324	9.861
2.110	5.604	4.352	11.28
3.866	5.337	4.352	13.21
6.599	5.199	4.340	14.25
11.87	5.141	4.327	16.07
22.31	5.075	4.414	18.97

points. The scaled energy $E_{\rm red}$ is defined to be zero at threshold, i.e., when $E_j=0$, and unity when $E_j=\infty$. The scaled collision strength $\Omega_{\rm red}(0)$ is the threshold value of Ω and $\Omega_{\rm red}(1)$ is given by[14]

$$\Omega_{\rm red}(1)=4w_i f_{ij}\frac{I_{\rm H}}{E_{ij}} , \tag{49}$$

where w_i is the statistical weight of level i, f_{ij} is the absorption oscillator strength, and $I_{\rm H}=13.6058$ eV. For an ion with a single outer electron the absorption oscillator strength is defined by

$$f(nl_a,n'l'_a)=\frac{l_{a>}}{3(2l_a+1)}B^2(nl_a,n'l'_a;1)\left[\frac{\Delta E}{I_{\rm H}}\right] , \tag{50}$$

where

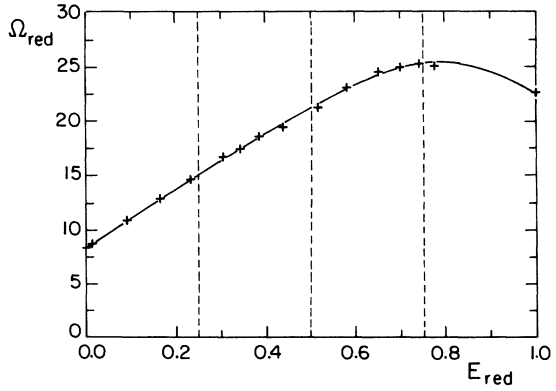

FIG. 1. Scale total collision strength $\Omega_{\rm red}^{\rm CDW\,II}$ for the $5s$-$5p$ transition in Sr^+ plotted against scaled energy $E_{\rm red}$. +, reduced data; ——, spline fit to the reduced data. Adjustable parameter $c=2.8$.

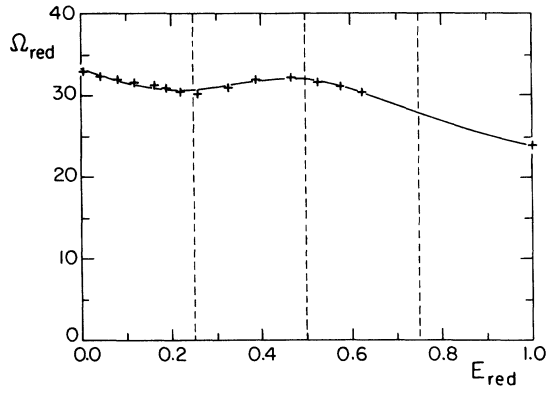

FIG. 2. Scaled total collision strength $\Omega_{\rm red}^{\rm CDW\,II}$ for the $4d$-$5p$ transition in Sr^+ plotted against scaled energy $E_{\rm red}$. +, reduced data; ——, spline fit to the reduced data. Adjustable parameter $c=8$.

$$B(nl_a,n'l'_a;1)=\int_0^\infty P_{nl_a}(r)rP_{N'l'_a}(r)dr , \tag{51}$$

$l_{a>}$ is the greater of l_a and $l'_{a>}$, ΔE is the transition energy, and the spin statistical weight factor 2 has been omitted in the degeneracy of the initial level $i=nl_a$ in Eq. (49). Consistent with such an omission is the neglect of the spin variable in Eq. (50), which gives the values $f(5s,5p)=1.265$ and $f(4d,5p)=0.107$ for the $5s$-$5p$ and $4d$-$5p$ transitions, respectively. For the quadrupolar transition $5s$-$4d$, Ω varies at high energies at $\Omega\sim$const and the data are reduced as[15]

$$E_{\rm red}=\frac{E_j/E_{ij}}{E_j/E_{ij}+c} , \tag{52}$$

$$\Omega_{\rm red}=\Omega . \tag{53}$$

Typical examples of the reduced data and spline fit to the

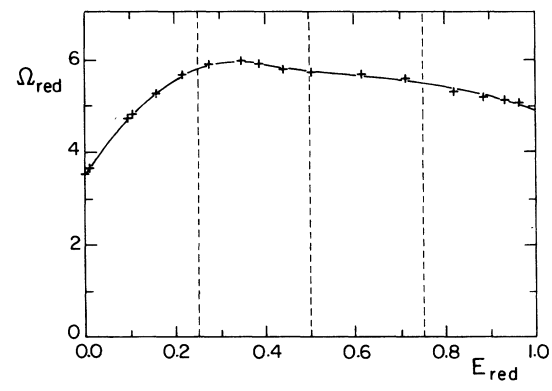

FIG. 3. Scaled total collision strength $\Omega_{\rm red}^{\rm CDW\,II}$ for the $5s$-$4d$ transition in Sr^+ plotted against scaled energy $E_{\rm red}$. +, reduced data; ——, spline fit to the reduced data. Adjustable parameter $c=6.3$.

TABLE V. Interpolated reduced collision strength Ω_{red} at the five energy knots, in the CDW II approximation, for the $5s$-$5p$, $4d$-$5p$, and $5s$-$4d$ transitions in Sr^+. Reduced energy E_{red}. The values of c have been chosen to optimize the distribution of data points.

E_{red}	$5s$-$5p$ $c=2.8$	$4d$-$5p$ $c=8$	$5s$-$4d$ $c=6.3$
0.0	8.346	33.23	3.503
0.25	15.02	30.94	5.797
0.50	21.15	32.02	5.776
0.75	25.28	27.94	5.500
1.00	22.54	23.82	4.938

reduced data are presented in Figs 1, 2, and 3 for the transitions $5s$-$5p$, $4d$-$5p$, and $5s$-$4d$, respectively. The values of Ω_{red}, in the CDW II approximation, at the five knots are tabulated in Table V. A graphical comparison of the original data (Ω) and the spline fit, which represents the data to an accuracy of a fraction of a percent, is shown in Figs. 4, 5, and 6 for the transitions $5s$-$5p$, $4d$-$5p$, and $5s$-$4d$, respectively.

Following a more traditional approach, we plot in Fig. 7 the excitation cross section for the $5s\ ^2S_{1/2}$-$5p\ ^2P_{3/2}$ transition in Sr^+ as a function of the colliding electron energy E. Our CDW II and CB II results are compared with the Coulomb-distorted two-state ($5s$-$5p$) calculations of Burgess and Sheorey[5] and the experimental results of Zapesochnyi *et al.*[6] The experimental data on the absolute excitation cross section of the resonance line of Sr^+ do not exclude the cascade transitions from the $6\ ^2S_{1/2}$ and $5\ ^2D_{3/2,1/2}$ levels to the $5S_{1/2}$ level. In Sr^+ there are two channels for the radiative decay of the $5p\ ^2P$ states: to the $5\ ^2S$ ground state and to the metastable ^4D ground states. The emission measurements were converted to excitation cross sections, using the experimental branching ratio of 0.936,[11] for the $5p$-$5s$ versus the $5p$-$4d$ decay modes. Zapesochnyi *et al.*[6] have given an

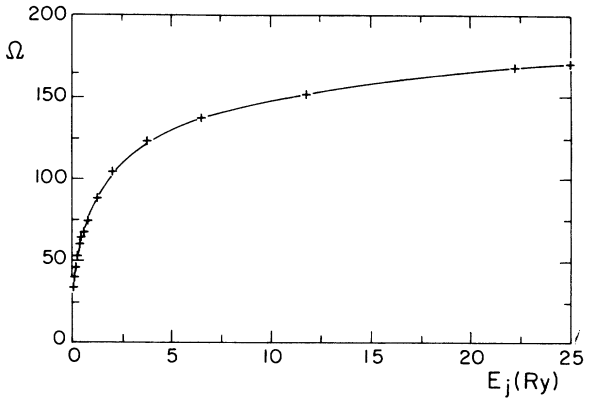

FIG. 5. Total collision strength $\Omega^{CDW\,II}$ for the $4d$-$5p$ transition in Sr^+ plotted against electron energy after excitation E_j. +, original data; ——, spline fit to the data.

experimental value for the $5s$-$5p$ excitation cross section at threshold of $32\pm6\times10^{-16}$ cm^2, which compares quite well with our CDW II result at threshold of 32.8×10^{-16} cm^2. The two-state calculations of Burgess and Sheorey,[5] on the other hand, overestimate the excitation cross section at threshold by 47%, which shows that the allowance for the $4d$ state, as we have done in our calculations, produces a large reduction in the total $5s$-$5p$ cross section. At slightly higher energies, our CDW II results are within 17% of the experimental values, and above 13 eV both sets of data differ by less than 5%. Burgess and Sheorey's results are in good agreement with these two cross sections for energies greater than 20 eV. Our CB II cross section lies above that of the CDW II approximation from threshold to 7 eV and slightly below for larger energies, until they merge at about 100 eV. For the $4d$-$5p$ and $5s$-$4d$ transitions we have been unable to find either experimental or theoretical results to compare with our calculations.

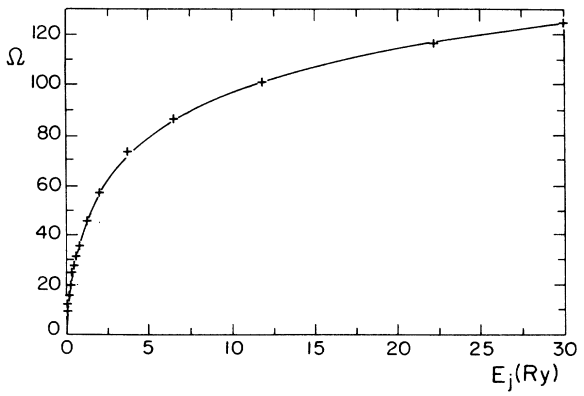

FIG. 4. Total collision strength $\Omega^{CDW\,II}$ for the $5s$-$5p$ transition in Sr^+ plotted against electron energy after excitation E_j. +, original data; ——, spline fit to the data.

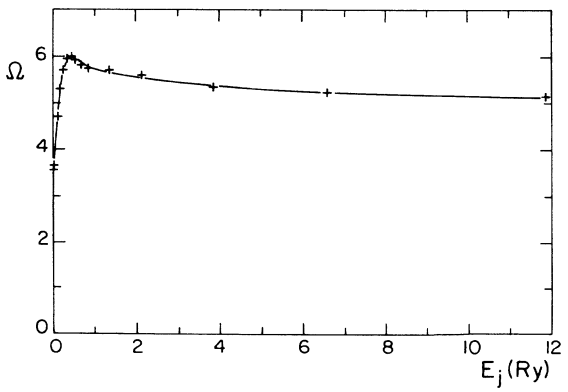

FIG. 6. Total collision strength $\Omega^{CDW\,II}$ for the $5s$-$4d$ transition in Sr^+ plotted against electron energy after excitation E_j. +, original data; ——, spline fit to the data.

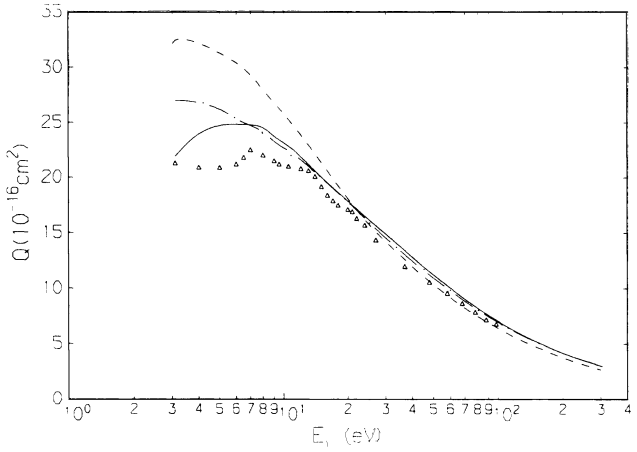

FIG. 7. Excitation cross section Q (10^{-16} cm^2) for the $5s\,^2S_{1/2}-5p\,^2P_{3/2}$ transition in Sr^+ plotted against incident electron energy E_i in eV. ——, present CDW II results; — — —, present CB II results; —·—·—·, two-state ($5s$-$5p$) distorted wave (Ref. 5); Δ, experimental points (Ref. 6).

V. CONCLUSIONS

The analysis of our CDW II calculations and comparison with other theoretical and experimental data, where available, suggest, on the whole, the validity of the following propositions.

(i) In the case of Sr^+, for the resonant transition $5s$-$5p$, the comparison between experiment and the present data seems to suggest that exchange does not play as important a role near threshold as it does in the case of Ca^+ ion[4] and the Mg^+ ion.[3] This is a tentative conclusion, drawn from the good agreement between the CDW II calculations, which neglect exchange, and the experimental data of Zapesochnyi *et al.*[6] Their measurements have yet to be confirmed by further and new investigations of the excitation of the resonant line of Sr^+.

(ii) The coupling of the $5s$ and $5p$ states to the $4d$ state has a drastic effect on the total $5s$-$5p$ excitation cross section at threshold. The allowance for the $4d$ state produces a large reduction in the total $5s$-$5p$ cross section.

(iii) For the optically forbidden transition $5s$-$4d$, the use of the analytic formula derived by the author[3] to estimate the contribution to the total collision strength from large values of angular momentum gives data with the correct high-energy behavior.

(iv) The new method for interpolating and assessing collision strengths developed by Burgess and Tully[15] corroborates the correctness of the behavior of our $5s$-$5p$, $4d$-$5p$, and $5s$-$4d$ collision strengths at high energies. Important advantages of their method are that the high-energy behavior of the collision strength is treated correctly by their program [see Eq. (49)] and printing and computational errors in the original data can be detected visually.

ACKNOWLEDGMENTS

This work was supported in part by the Natural Sciences and Engineering Research Council of Canada. I am grateful to A. Burgess for the processing of the present data and for permission to quote the results prior to the publication of the method.

[1] *Astrophysics and Space Science Library 125, Upper Main Sequence Stars with Anomalous Abundances, Proceedings of the 90th Colloquium of the International Astronomical Union,* edited by C. R. Cowley, M. M. Dworetsky, and C. Megessier (Reidel, Dordrecht, 1986).

[2] *Astrophysics and Space Science Library 114, Cool Stars with Exceeses of Heavy Elements, Proceedings of the Strasbourg Observatory Colloquium,* edited by M. Jaschek and Ph.C. Keenan (Reidel, Dordrecht, 1985).

[3] M. C. Chidichimo, Phys. Rev. A **37**, 4097 (1988).

[4] M. C. Chidichimo, J. Phys. B **14**, 4149 (1981).

[5] A. Burgess and V. B. Sheorey, J. Phys. B **7**, 2403 (1974).

[6] I. P. Zapesochnyi, V. A. Kel'man, A. I. Imre, A. I. Dashchenko, and F. F. Danch, Zh. Eksp. Teor. Fiz. **69**, 1948 (1975) [Sov. Phys.—JETP **42**, 989 (1976)].

[7] I. C. Percival and M. J. Seaton, Proc. Cambridge Philos. Soc. **53**, 654 (1957).

[8] A. Burgess, J. Phys. B **7**, L364 (1974).

[9] C. E. Moores, *Atomic Energy Levels,* Nat. Bur. Stand. Ref. Data Ser., Natl. Bur. Stand. (U.S.) Circ. No. 35 (U.S. GPO, Washington, D.C., 1971), Vol. II, p. 191.

[10] A. Burgess (private communication).

[11] A. Gallagher, Phys. Rev. **157**, 24 (1967).

[12] A. Burgess, H. E. Mason, and J. A. Tully, in International Astronomical Union Colloquium No. 102 on UV and X-ray Spectroscopy of Astrophysical and Laboratory Plasmas (1988) [J. Phys. (Paris) Colloq. **49**, C1-107 (1988)].

[13] A. Burgess (unpublished).

[14] A. Burgess and J. A. Tully, J. Phys. B **11**, 4271 (1978).

[15] A. Burgess and J. A. Tully (unpublished).